Journal of
Mechanical
Science and
Technology

Journal of Mechanical Science and Technology 21 (2007) 1534~1540

Instability map based on specific plastic work criterion for hot deformation

H. W. Lee[1], H. C. Kwon[2], M. Awais[1] and Y. T. Im[1,*]

[1]*National Research Laboratory for Computer Aided Materials Processing, Department of Mechanical Engineering, Korea Advanced Institute of Science and Technology, 373-1, Gusongdong, Yusonggu, Daejeon, 305-701, Korea*
[2]*Rolling Technology and Process Research Group, POSCO Technical Research Laboratories, Pohang 790-785, Korea*

(Manuscript Received May 31, 2007; Revised August 30, 2007; Accepted September 30, 2007)

Abstract

Estimating workability is very important to complete the hot or cold working process successfully without making any crack. Instability map was developed by utilizing conventional plastic work criterion in the current study. Hot compression tests were conducted using Gleeble 3800 simulator to obtain flow stress curves as a function of temperature and strain rate. Based on the compression results, new instability map based on the specific plastic work was developed for estimating the instability during the hot deformation process. The critical specific plastic work value was determined by investigating the surface irregularity and shear band formation in the compressed specimens. Then, the instability map determined was applied for predicting surface wrinkle defect during the multi-pass hot bar rolling in combination with the finite element analysis. The predicted results using new instability map suggested matched well with the observations obtained from the industry. The developed approach is easy to apply to the available simulation tools to determine necessary processing parameters.

Keywords: Instability map; Plastic work; Surface wrinkle defect; Finite element analysis

1. Introduction

Workability is concerned with the extent to which a material can be deformed in a specific metalworking process without the formation of cracks [1]. According to type of the process, the limit of workability can be determined differently by the formation of local necking, shear band, and surface irregularity. Workability is affected not only by the material characteristics such as grain size, distribution of second phase, and specimen geometry but also by process characteristics such as strain, strain rate, and temperature.

Therefore, the parameter for estimating the workability should be considered from both characteristics. In cold working processes, the process characteristics play a major role to decide the workability due to inactive metallurgical phenomenon, and both characteristics make an effect on workability for hot working processes.

Many ductile fracture criteria were suggested and used for investigation of the workability in cold working processes [2, 3]. Clift et al. [2] examined these ductile fracture criteria in cold deformation using the finite element method and experimental results. Kim et al. [3] predicted ductile fracture in multi-stage cold forging of aluminum alloy using ductile fracture criteria of specific plastic work and Cockroft and Latham.

The workability or instability in hot working processes has also been dealt with by many resear-

*Corresponding author. Tel.: +82 42 869 3227, Fax.: +82 42 869 3210
E-mail address: ytim@kaist.ac.kr

chers. Crowther and Mintz [4] analyzed the change of hot ductility with respect to working temperature and carbon contents using hot tensile tests. Raj [5] suggested processing map by representing the condition for cavity nucleation, dynamic recrystallization, and adiabatic heating as a function of temperature and strain rate with atomistic point of view. However, this atomistic theory is difficult to apply for finite element analysis based on continuum theory. Semiatin and Lahoti [6] suggested the flow localization parameter based on force equilibrium principle and applied it to the finite element analysis to determine the flow instability. Prasad et al. [7] developed dynamic material model (DMM) which considered the material during hot deformation as power dissipator. Later, Prasad and Sasidhara [8] suggested the instability map to check hot workability with the superposition of power dissipation map. Malas and Seetharaman [9] suggested flow instability criterion based on the DMM theory. Kopp and Bernrath [10] suggested and determined forming limit curves by using the compression test with carbon steel specimen with various geometries. However, there is still no widely accepted approach to estimate hot workability or instability of the material.

Thus, conventional plastic work approach, generally used as a ductile fracture criterion in the cold working process, was reconsidered as instability criterion to predict the surface wrinkle defect during the multi-pass hot bar rolling in the current study. For this investigation, hot compression tests under various temperatures and strain rates were conducted using Gleeble 3800 machine. From the stress-strain curves obtained, the specific plastic work value for a specific strain, strain rate, and temperature was calculated and represented as an instability map.

The polished and etched cross sections were compared in terms of the surface irregularity and shear band formation to determine the critical specific plastic work value representing the limit of workability or initiation of instability. Then, instability maps derived were applied to predict surface wrinkle defect during the multi-pass hot bar rolling of carbon steel in combination with the finite element analysis. The simulation results were in a reasonably good agreement with industrial observations.

2. Experimental

Two types of steel were used for the current investigation and their chemical compositions are given in Table 1. Compression specimen with a height of 15 mm and a diameter of 10 mm was prepared by machining.

Table 1. Chemical compositions of the steel used.

weight%	C	Si	Mn	P	S	Cu	Al
Steel A	0.090	0.028	0.458	0.014	0.005	0.009	0.062
Steel B	0.378	0.226	0.734	0.014	0.010	0.008	0.032

A series of hot compression tests was conducted at constant strain rate from 0.1 to 10 for steel A and from 0.01 to 100 for steel B. The deformation temperatures were varied from 500 to 1000 °C for steel A and from 500 to 1100 °C for steel B at 100 °C increments. The tantalum foil was used between the specimen and dies to prevent sticking between them. The thermocouple was attached by welding at the midspan to provide feedback control and measurement during experiments.

Specimen was resistance heated to deformation temperature at a heating rate of 10 °C/sec and homogenized for 60 sec before initiating compression. The deformed specimen was water quenched after 60 % reduction in height and time delay was about 2 sec. The quenched specimens were sectioned in compression direction and polished for further observation using optical microscopy.

3. Results and discussion

3.1 Analysis of Flow Stress Curves

Fig. 1 shows the true stress-strain curves for different temperatures and strain rates for steel A and B. For steel A, at the temperature of 900 °C, the flow curves represent softening behavior after peak stress due to dynamic recrystallization and recovery at lower strain rates such as 0.1, 0.5, and 1 sec^{-1} and steady state flow at higher strain rates of 5 and 10 sec^{-1} as shown in Fig. 1(a). The flow curves obtained for steel A at 1 sec^{-1} at different temperatures ranging from 500 to 1000 °C are presented in Fig. 1(b). The flow curves with temperatures of 500, 600, 700, and 800 °C show steady state flow due to dynamic recovery. For higher temperatures of 900 and 1000 °C, softening behavior after peak stress was revealed by initiation of dynamic recrystallization.

For steel B, Fig. 1(c) and (d) show the effect of strain rate and temperature on flow curves, respectively. Flow softening after peak stress was shown

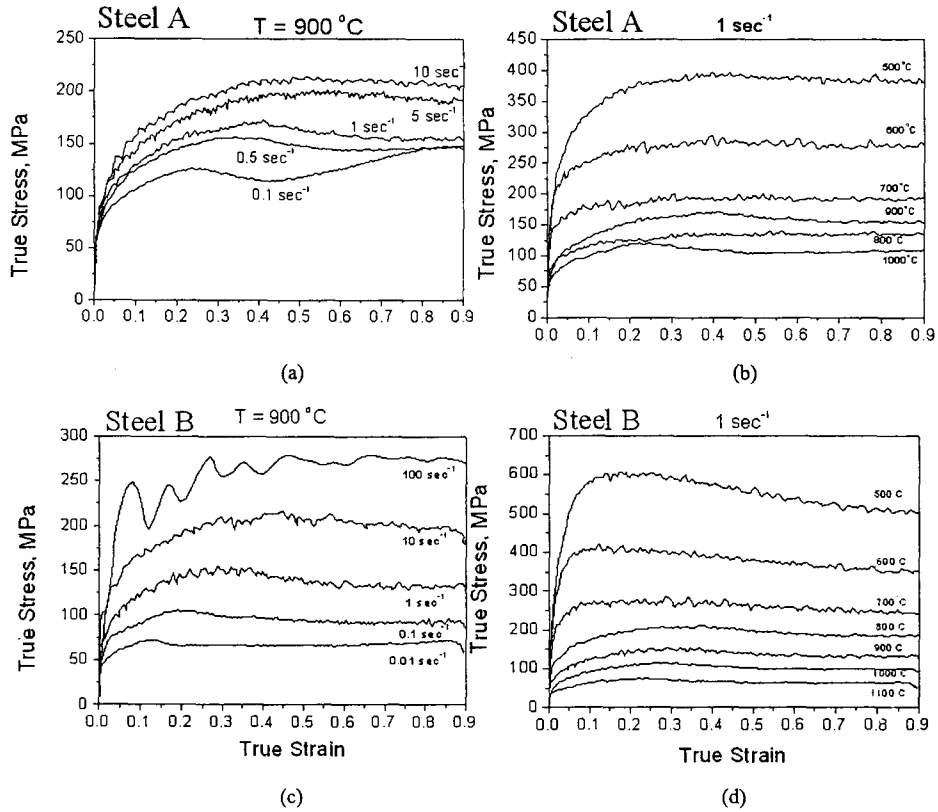

Fig. 1. Flow curves of steel A and B for various strain rates at 900 °C and various temperatures at 1 sec^{-1}, respectively.

clearly at lower strain rates of 0.01, 0.1, and 1 sec^{-1}. For higher strain rates of 10 and 100 sec^{-1}, the flow curves show almost steady state flow. The large fluctuation of flow for strain rate of 100 sec^{-1} was mostly due to measurement error because of fast compression speed. For steel B with the strain rate of 1 sec^{-1}, the flow curves represent softening behavior after peak stress due to dynamic recrystallization and recovery at higher temperatures of 800, 900, 1000, and 1100 °C. For lower temperatures of 500, 600, and 700 °C was observed steady decrease due to dynamic recovery.

The stress levels of steel A and B were higher with higher strain rate for all conditions. The stress levels of steel A and B were mostly higher with lower temperature except for steel A with the temperature of 800, 900, and 1000 °C. It was due to changing of dominant mechanism from recovery to recrystallization by increasing the temperature. However, this rule was preserved in the temperature range from 500 to 800 °C and from 900 to 1000 °C in which the dominant mechanism was the same.

3.2 Development of new instability map

In cold working processes, the ductile fracture criteria by Cockcroft-Latham and plastic work have been widely used for predicting the position and initiation of possible crack. The Cockcroft-Latham criterion is integration of maximum tensile stress with respect to the strain. The specific plastic work is represented as integration of effective stress with respect to effective strain. The Cockcroft-Latham criterion assumes that the crack was initiated by tensile stress and considers direction of stress as a critical factor. The amount of deformation energy is more important than direction of the stress in hot working processes because many metallurgical phenomena are involved to dissipate the accumulated deformation energy. The plastic work criterion represents the amount of deformation energy. The effective stress is a function of temperature, strain, strain rate, and grain size and affected by metallurgical phenomena indirectly. For example, the total amount of deformation energy can be decreased with recrystallization due to softening, and the

formation of instability such as crack, shear band, and surface irregularity will be decreased.

Therefore, the specific plastic work value was employed as a criterion to estimate the instability of metals for hot working processes in the current study as follows:

$$C_1 = \int \bar{\sigma}\ d\bar{\varepsilon} \tag{1}$$

where $\bar{\sigma}$ is the effective stress and $\bar{\varepsilon}$ the effective strain.

The specific plastic work for each temperature, strain, and strain rate values were calculated from flow curves by calculating the area under the flow curve. The specific plastic work values were calculated for the strain ranging from 0.3 to 0.8 and the values for the strain 0.6 are shown in Table 2. The specific plastic work values for steel B are larger than those of steel A at the temperature of 500 to 800 °C because of its higher stress levels.

To represent the specific plastic work values, contour plot of specific plastic work respect to temperature and strain rate for steel A and B can be made for the strain of 0.3 to 0.8 and the plot with strain 0.6 is shown as an example in Fig. 2. The contour levels indicate the specific plastic work C_1. As shown in this figure, the specific plastic work value is generally larger with low temperature and larger strain rate because of higher values of the stress.

3.3 Determination of the critical value

To determine the critical specific work value of steel A and B, compression specimen was sectioned at the symmetry plane and polished to observe the

Table 2. Calculated specific plastic work values at the strain of 0.6.

	Temperature / Strain rate	500	600	700	800	900	1000	1100
Steel A	0.1	205.2	138.8	87.3	57.1	68.5	45.9	-
	0.5	211.1	154.8	98.3	70.8	83.6	59.2	-
	1	217.7	162.6	111.2	75.8	91.1	63.9	-
	5	233.6	192.5	131.8	91.2	104.3	81.1	-
	10	231.9	183.7	146.3	97.0	111.9	86.9	-
Steel B	0.01	268.6	173.1	97.5	61.5	39.3	26.8	16.5
	0.1	315.8	213.4	128.6	86.4	56.5	39.8	25.0
	1	333.5	230.8	156.7	113.6	80.6	60.2	39.3
	10	378.1	291.4	198.6	148.0	114.0	85.2	60.2
	100	412.6	365.9	256.1	196.5	146.9	113.4	87.1

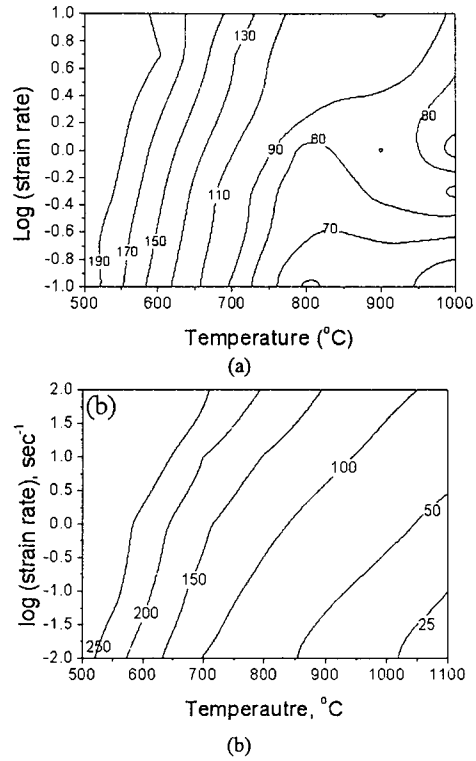

Fig. 2. Contour plot of specific plastic work for steel A and (b) steel B.

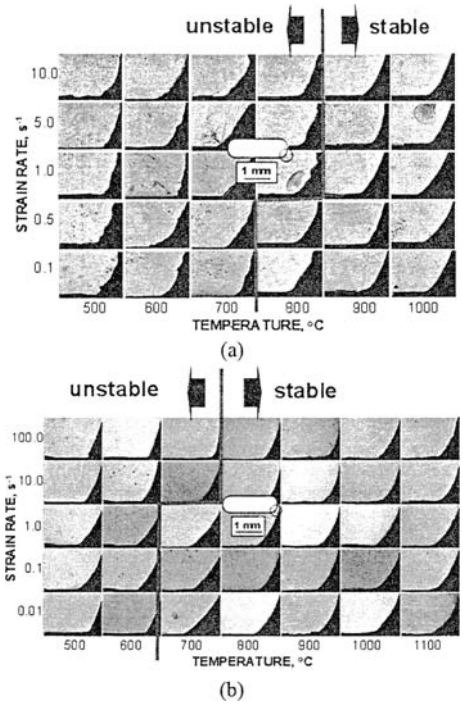

Fig. 3. Sectioned surface profiles of compressed specimen of (a) steel A and (b) steel B.

surface quality and shear band formation with optical microscopy. In Fig. 3, the surfaces of the specimen at lower temperatures and higher strain rates were wavy for steel A. These wavy surfaces can be explained in the view point of energy dissipation. To keep equilibrium, the material under deformation has to dissipate energy in some ways. At high temperature range, the deformation energy mostly dissipates by recrystallization. However, the deformation energy dissipates by creating extra surface at low temperature due to absence of recrystallization.

The wavy surface was clearly shown for steel A than steel B. It means that the steel B has better workability compared to steel A. Therefore, the stable and unstable flow can be easily separated for steel A by comparing the surface profile shown in Fig. 3(a). However, it is not easy to separate the stable and unstable flow for steel B because the compressed

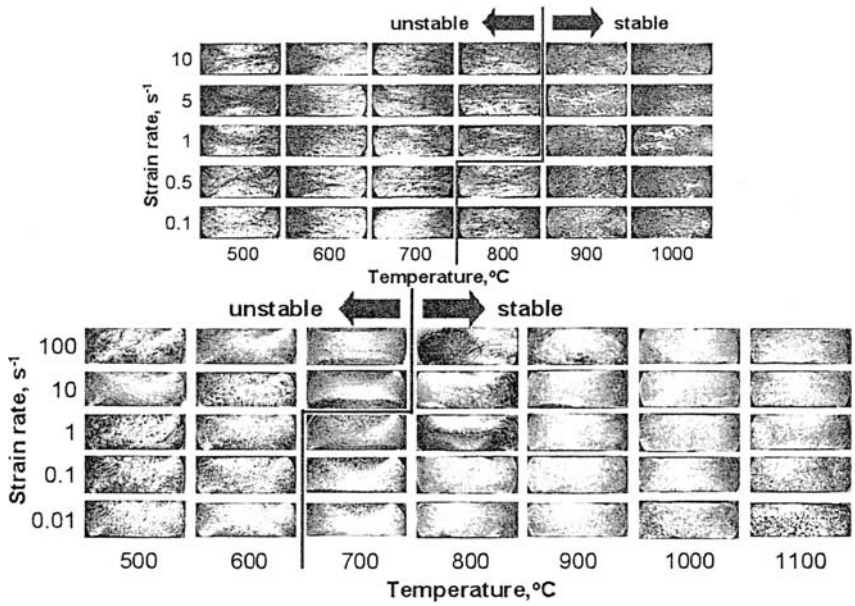

Fig. 4. Metal flow of compressed specimens of (a) steel A and (b) steel B.

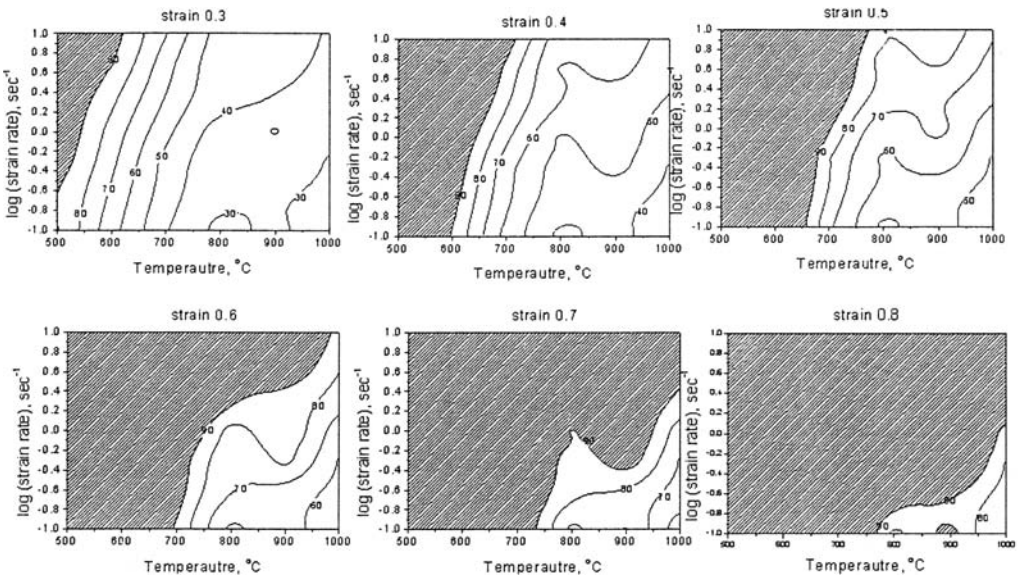

Fig. 5. Instability map of steel A.

specimens of steel B have relatively clear surfaces for most of cases.

Therefore, metal flows of steel A and B were also observed to check the instability with optical microscopy as shown in Fig. 4. For both steels, flow localization in terms of shear band was observed at low temperature and high strain rate range. The flow localization reduced workability of the steel by inducing the shear band formation, single or double.

Based on these observations, the critical value was decided to be 90 for steel A and 190 for steel B by averaging the specific plastic work value at the border of stable and unstable region in Figs. 3 and 4. In the current study, the critical value was determined based on surface irregularity and flow instability of shear deformation since the surface wrinkle defect that was mostly happened due to surface flow instability was the major issue involved.

The developed instability maps of steel A and B for various strain ranges are given in Figs. 5 and 6, respectively. In this figure, contour levels indicate the specific plastic work C_1 and the hatched area represents the unstable area. Steel A shows larger unstable area than steel B at the same condition. It means that steel B has better workability compared to steel A as mentioned earlier. Both steel A and B show higher specific plastic work value for lower temperature and higher strain rate region although the specific value and region are different.

3.4 Validation of the instability map

The instability maps obtained at different strains were implemented into the CAMP*roll*, which was developed based on rigid-thermo-viscoplastic approach [11]. The finite element (FE) simulations were aimed to check the applicability of current approach to the multi-pass hot bar rolling process.

In the FE analysis, the flow stress of the material

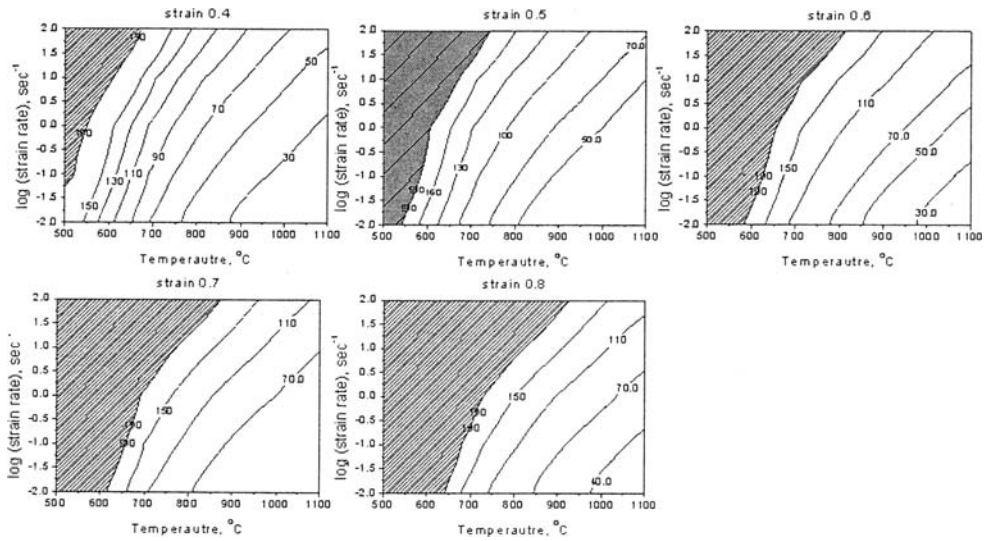

Fig. 6. Instability map of steel B.

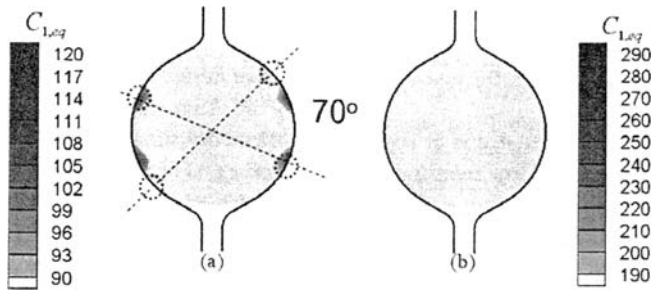

Fig. 7. Predicted position of surface wrinkle defect for (a) steel A and (b) Steel B.

represented in Fig. 1 was modeled with the power law, $\bar{\sigma} = C(\bar{\varepsilon}, T)\dot{\bar{\varepsilon}}^m$ for non-isothermal simulations. The strength coefficient (C) and strain rate sensitivity (m) were provided in a tabular form at constant temperatures and strain values. The constant shear friction factor of 0.6 was used in simulations. The interface heat transfer coefficient between the workpiece and rolls of 3 kW/m^{2}K was used. The roll and room temperatures were assumed to be 60 and 25 °C, respectively.

The FE result shown in Fig. 7 was compared with the industrial mill observation available in the literature [12]. In the industrial mill observation, the surface defect mostly happened for steel A rather than steel B. In addition, the position of surface defect after the pass 5 for steel A was at the area , represented as a dotted circle in the figure, surface of the billet that is 35° rotated from the eccentric horizontal line.

In Fig. 7(a), the unstable area (dark grey area) is at the position 35° rotated from the horizontal center line. It is almost the same as the experimental observation by neglecting the eccentricity that was observed in industry due to rotation of the billet according to the torsional effect. For steel B, result also shows no unstable area like the observation as expected due to better workability.

From the above investigation, new instability map looks valid to determine the processing condition to induce the surface wrinkle defect during the multi-pass hot bar rolling.

4. Conclusion

In the present investigation, new instability map based on the specific plastic work was suggested for estimating the instability. The developed approach was applied to predict the surface defect during the multi-pass hot bar rolling of steels. The results can be summarized as follows:

The observation of flow curves obtained from the hot compression test showed that the dominant deformation mechanisms of steel A and B were dynamic recovery for high strain rate and low temperature and dynamic recrystallization for low strain rate and high temperature.

Instability maps obtained for steel A and B show unstable area at high strain rate and low temperature range.

Finite element results indicated that unstable regions were at the place which was 35° rotated from the horizontal center line, where surface cracks were observed in industry.

Acknowledgements

The authors wish to thank for the grants from the POSCO and Korea Science and Engineering Foundation (KOSEF) through the National Research Laboratory Program funded by the Ministry of Science and Technology (No. R0A-2006-000-10240-0). The technical support of the POSCO to carrying out the hot compression tests was very much appreciated.

References

[1] G.E. Dieter, Mechanical metallurgy, McGracw-Hill, Inc. (1976).

[2] S.E.Clift, P. Hartely, C.E.N. Strugess, G.W. Rowe, Fracture prediction in plastic deformation processes, *Int. J. Mech. Sci.* 32 (1990) 1-17.

[3] H.S. Kim, Y.T. Im, M. Geiger, Prediction of ductile fracture in cold forging of aluminum alloy, *J. Manuf. Sci. Eng.* 121 (1999) 336-344.

[4] D.N. Crowther and B. Mintz, Influence of carbon in hot ductility of steels, *Mater. Sci. Technol.* 2 (1986) 671-676.

[5] R. Raj, Development of a processing map for use in warm-forming and hot-forming processes, *Metall. Trans. A.* 12 (1981) 1089-1097.

[6] S.L. Semiatin and G.D. Lahoti, Deformation and unstable flow in hot torsion of Ti-6Al-2Sn-4Zr-2Mo-0.1Si, *Metall. Trans. A,* 12 (1981) 1719-1728.

[7] Y.V.R.K. Prasad, H.L. Gegel, S.M. Doraivelu, J.C. Malas, J.T. Morgan, K.A. Lark, D.R. Barker, Modeling of dynamic material behavior in hot deformation: forging of Ti-6242, *Metal. Trans. A.* 15 (1984) 1883-1992.

[8] Y.V.R.K. Prasad and S. Sasidhara, Hot working guide- A compendium of processing maps, *ASM International*, Ohio, 1997.

[9] J.C. Malas, V. seethataman, Using material behavior models to develop process control strategies, *JOM.* 44 (1992) 8-13.

[10] R. Kopp and G. Bernrath, The determination of formability for cold and hot forming conditions, *Steel Research.* 70 (1999) 147-153

[11] S.Y. Kim and Y.T. Im, Three-dimensional finite element simulation of non-isothermal shape rolling, *J. Mater. Process. Technol.* 127 (2002) 57-63.

[12] H.C. Kwon, H.W. Lee, H. Y. Kim, Y.T. Im, H.D. Park, D.L. Lee, Surface defect in the hot bar rolling process of carbon steel, Internal report, 2007.